Quantum Electronics **36** (9) 883–888 (2006)

LASER APPLICATIONS AND OTHER TOPICS IN QUANTUM ELECTRONICS

PACS numbers: 41.20.Jb; 52.35.Hr
DOI: 10.1070/QE2006v036n09ABEH013290

Reflection of an electromagnetic pulse from a subcritical waveguide taper and from a supercritical-density plasma in a waveguide

A.A. Rukhadze, V.P. Tarakanov

Abstract. **Two related problems are studied by numerical simulations using the KARAT code: the reflection of the TM_{01} mode of an electromagnetic pulse from the subcritical taper of the section of a circular waveguide and the reflection of the same pulse from a 'cold' collisionless plasma with a density increasing up to a supercritical value along the waveguide axis. It is shown that in the former case the pulse is totally reflected with an insignificant distortion of its shape, in accordance with the linear theory. In the latter case, the character of reflection depends substantially on the plasma density increase length, the pulse duration, and the wave field amplitude, a significant field deceleration and amplitude growth occurring near the critical point; the pulse absorption in the plasma far exceeds the absorption due to the linear transformation of the incident transverse wave to the longitudinal plasma oscillations.**

Keywords: *electromagnetic pulse, reflection of electromagnetic waves, metal waveguide, nonuniform plasma.*

1. Introduction

This study was initiated by the recently published paper [1] in which the reflection of a monochromatic wave from the critical point of a waveguide was considered. The group velocity of the wave decreases sharply near the critical point, which should, in the author's opinion [1], lead to the unlimited growth of the incident-wave amplitude, the broadening of its frequency spectrum, and the formation of a shock-like wave. These statements raised our doubts, and we numerically simulated the reflection of a TM-mode microwave radiation pulse from the tapering part of a waveguide with the help of the KARAT code [2] using the only restriction by retaining the boundary condition of the ideal metal waveguide surface.* We revealed no significant deviations from linear electrodynamics, the field amplitude enhancement in the vicinity of the critical point not exceeding a factor of two, which corresponds to the linear theory of wave reflection from a metal surface, i.e. the unlimited field growth and the production of a shock-like wave were not observed. The results of numerical simulations of this problem and a comment to them are given in Section 2.

The second problem – that of the TM-mode reflection from the plasma which fills a waveguide of constant radius where the density rises to a supercritical value – is of substantially greater interest. In this case, near the critical point, where the plasma frequency coincides with the wave frequency, the group velocity of the wave becomes lower, which should result in the field enhancement. Because the plasma is an inherently nonlinear medium, nonlinearities in this region should be particularly strongly pronounced. Note that V.L. Ginzburg [3] draw attention to the enhancement of the longitudinal field in the vicinity of the critical point upon oblique incidence of an electromagnetic wave on the surface of a cold nonuniform-density plasma (this effect was noted even in monograph [4]).

It was shown in Ref. [5] that at the point of resonance enhancement (which is referred to as plasma resonance) a longitudinal plasma wave was excited, resulting in a partial absorption of the electromagnetic wave incident on the plasma. Subsequently, this effect was intensively studied (see reviews [6, 7]) and was called the linear transformation of a transverse wave to a longitudinal wave in the nonuniform plasma at the point of plasma resonance. The absorption of the electromagnetic wave at the point of plasma resonance essentially depends on the plasma density gradient and attains a maximum when the characteristic density gradient scale is comparable with the wavelength of the incident wave.

In Section 3, the linear wave transformation theory is generalised to the case of the TM_{01}-mode reflection from the plasma in a waveguide; we give the results of numerical simulation of this problem, which takes into account the plasma density gradient, the plasma nonlinearity for a finite amplitude of the wave incident on the plasma, as well as the limited duration of the pulse.

In Section 4, the results of numerical simulations are compared with the results of the linear theory of wave transformation at the point of plasma resonance. A significant discrepancy between them, in our opinion, is due to the accumulation of the field in the region of plasma resonance and to the manifestation of nonlinear effects in the plasma.

*We thereby neglected the nonlinear damping at the waveguide walls, keeping only the possibility for broadening of the spectrum and distortion of the pulse shape of the incident wave.

A.A. Rukhadze A.M. Prokhorov General Physics Institute, Russian Academy of Sciences, ul. Vavilova 38, 119991 Moscow, Russia; e-mail: rukh@fpl.gpi.ru;
V.P. Tarakanov Scientific Association for High Temperatures, Russian Academy of Sciences, ul. Izhorskaya 13/19, 127412 Moscow, Russia

Received 28 March 2006; revision received 22 May 2006
Kvantovaya Elektronika **36** (9) 883–888 (2006)
Translated by E.N. Ragozin

2. Reflection from the subcritical taper of a circular waveguide

Numerical simulations were performed by using the KARAT code [2], which enabled solving the complete system of Maxwell equations on shifted grids by an explicit finite-difference technique correct to the second order.

A TM_{01}-polarised pulse (with nonzero field components E_z, E_r, and B_φ) with a carrier frequency $f = 10$ GHz and a duration of ~ 1 ns is injected into a metal waveguide of length $L = 80$ cm and of radius $R = 2$ cm at the input. Beginning with $z = 40$ cm, the waveguide radius decreases linearly to 0.2 cm for $z = 80$ cm (the geometry is shown in Fig. 1).

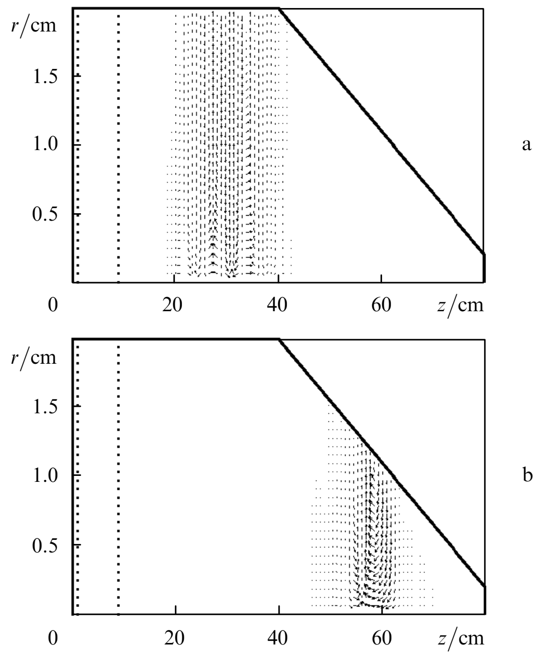

Figure 1. Vector field in the metal waveguide before reflection (a) and at the instant of its deepest penetration into the waveguide (b). The solid line indicates the waveguide boundaries, at the left (the dotted lines) is the window with the boundary conditions for the input and output of the wave, close short lines (arrows) stand for the net electric field.

Figures 1a and 1b show the vector field of the wave prior to reflection and at the instant of its deepest penetration into the waveguide. The field amplitude at the instant of reflection is two times higher than the amplitude of the incident wave, which corresponds to the linear theory.

Figure 2 shows the dynamics of the Poynting vector during the propagation of an electromagnetic pulse through the section for $z = 20$ cm. One can see that at first the 1-ns pulse propagates and then the reflected electromagnetic wave appears. The total energies of the incident and reflected pulses are equal. The pulse shape almost does not change.

This picture is in complete agreement with the linear theory of wave reflection from a metal mirror [8], i.e. the doubling of incident wave amplitude at the mirror surface without the formation of a shock-like wave near the critical point. This was to be expected, because both the field equations and the boundary conditions at the waveguide surface are linear and there are no grounds to expect the occurrence of nonlinear effects.

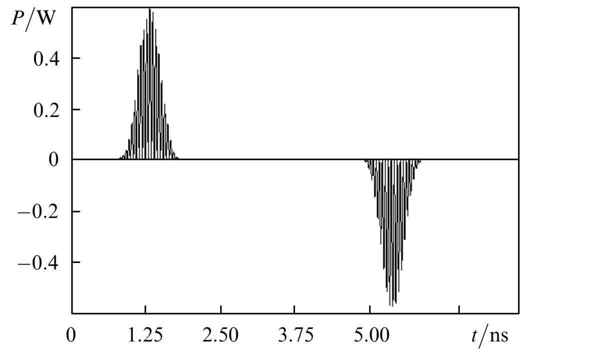

Figure 2. Poynting vectors of the incident and reflected waves during the propagation of an electromagnetic pulse through the waveguide section at $z = 20$ cm.

3. Reflection from the plasma in a waveguide with a density increasing to a supercritical value

The second problem consists in the investigation of reflection of the same pulse from a plasma with a density increasing to the supercritical value. The plasma fills the waveguide, beginning from $z = 40$ cm, and its density increases linearly over a length L up to the maximum value $n_{\max} = 2.5 \times 10^{12}$ cm^{-3} (or 10^{13} cm^{-3}) and then remains constant. In our calculations, the length L was varied from zero to 20 cm, the pulse duration was varied from 0.2 to 1.0 ns, and the incident wave field intensity from 5 to 5×10^4 V cm^{-1}. These parameters were varied to investigate the effect of the maximum plasma density, the density gradient, the field amplitude, and the pulse duration on the type of reflection of the TM_{01} waveguide mode. All of them have a substantial effect on the features of wave reflection from the critical-density plasma and on the absorption of the incident wave in the plasma.

3.1 Analytical theory of reflection

Before discussing the results of numerical simulations, we consider the linear approximate analytic theory of electromagnetic wave reflection from the critical point in a plasma with increasing density. We will follow Ref. [5] (see also Ref. [9]) by generalising calculations to the cylindrical geometry.

We assume that the circular metal waveguide of radius R does not contain plasma for $z \leqslant 0$ (region I). For $0 < z < L$ (region II), the plasma density increases to

$$N_{\max} > N_{\rm cr} = \frac{m\omega^2}{4\pi e^2},$$

where m and e are the electron mass and charge; $\omega = 2\pi f$ is the frequency of the pulse incident on the plasma. For $z \geqslant L$ (region III), the plasma density is constant, $N = N_{\max}$.

As mentioned above, we consider the propagation of the fundamental axially symmetric TM mode with E_z, E_r, and B_φ nonzero field components. In this case,

$$E_r = -\frac{\mathrm{i}c}{\omega\varepsilon}\frac{\partial B_\varphi}{\partial z}, \quad E_z = \frac{\mathrm{i}c}{\omega\varepsilon}\frac{1}{r}\frac{\partial}{\partial r}rB_\varphi,$$
$$\varepsilon(z)\frac{\partial}{\partial z}\frac{1}{\varepsilon(z)}\frac{\partial B_\varphi}{\partial z} + \frac{\partial}{\partial r}\frac{1}{r}\frac{\partial}{\partial r}rB_\varphi + \frac{\omega^2}{c^2}\varepsilon(z)B_\varphi = 0. \qquad (1)$$

Here,

$$\varepsilon(z) = 1 - \frac{\omega_{\rm p}^2}{\omega^2} \qquad (2)$$

is the plasma permittivity; $\omega_{\rm p}^2 = 4\pi e^2 N(z)/m$; and $N(z)$ is the longitudinally nonuniform plasma density. Equation (1) is applicable throughout the entire range of z values, i.e. outside the plasma (for $z < 40$ cm), in the density increase region ($0 \leqslant z \leqslant L$), and in the region $z > 40$ cm, where the plasma is uniform and possesses the highest density equal to $N_{\max}$. It can be easily shown that the solution of Eqn (1) satisfying the boundary conditions at the side surface of the metal waveguide can be written as

$$B_\varphi(z, r) = B(z) J_1\left(\frac{\mu r}{R}\right), \qquad (3)$$

where $\mu \simeq 2.41$ and $B(z)$ satisfies the equation

$$\varepsilon \frac{\partial}{\partial z}\left(\frac{1}{\varepsilon}\frac{\partial B}{\partial z}\right) - \frac{\mu^2}{R^2} B + \frac{\omega^2}{c^2}\varepsilon B = 0. \qquad (4)$$

In region I,

$$B(z) = C_{\rm in}\exp(-{\rm i}\omega t + {\rm i}k_{z1}z) + C_{\rm out}\exp(-{\rm i}\omega t - {\rm i}k_{z1}z), \qquad (5)$$

where $C_{\rm in}$ and $C_{\rm out}$ are the amplitudes of the incident and reflected waves.

In region III (supercritical-density plasma), the wave does not propagate and

$$B(z) = C_{\rm tr}\exp(-{\rm i}\omega t - {\rm i}k_L z), \quad k_L^2 = \frac{\mu^2}{R^2} - \frac{\omega^2}{c^2}\varepsilon. \qquad (6)$$

In region II (the plasma with increasing density) there is a point of plasma resonance; for $f = 10$ GHz, at this point

$$\omega_{\rm p}^2(z) = \omega^2 \approx 3.94 \times 10^{21}\ {\rm s}^{-1}. \qquad (7)$$

Let us next consider the limiting case $\lambda = c/f > L$ (a rapid density growth), when Eqn (4) can be solved by following Ref. [9], i.e. assuming the second and third terms to be small. In the region of plasma resonance for $0 \leqslant z \leqslant L$ we obtain (see Ref. [9], exercise 1 in Chapter VII)

$$B_\varphi(0, r) = B_\varphi(L, r) = C J_1\left(\frac{\mu r}{R}\right),$$

where C is an arbitrary constant determined from the boundary conditions

$$E_r(L, r) = E_r(0, r) + \frac{c\pi}{\omega} B_\varphi(0, r)\frac{\mu^2}{R^2}\eta, \qquad (8)$$

where $\eta^{-1} = |{\rm d}\varepsilon/{\rm d}z|$, with $E_r(z, r) \propto J_1(\mu r/R)$. By sewing together the solution in the region $0 \leqslant z \leqslant L$ and the evanescent solution for $z > L$, we obtain

$$E_r(L, r) = \frac{{\rm i}\kappa_L c}{\omega} B_\varphi(L, r) = \frac{{\rm i}\kappa_L c}{\omega} B_\varphi(0, r), \qquad (9)$$

where κ_L is the field attenuation coefficient in the region $z > L$;

$$\kappa_L^2 = \frac{\mu^2}{R^2} - \frac{\omega^2}{c^2}\varepsilon > 0. \qquad (10)$$

Finally we obtain

$$E_r(0, r) = \frac{c}{\omega}\left(\frac{{\rm i}\kappa_L}{\varepsilon} + \eta\frac{\pi\mu^2}{R^2}\right) B_\varphi(0, r) = \frac{c}{4\pi} Z(0, r) B_\varphi. \qquad (11)$$

Here, $Z(0, r)$ is the surface impedance of the reflective plasma layer (with increasing density), which is related to the complex amplitude reflectivity for the TM wave:

$$\mathscr{R} = -\left[1 - \frac{\omega}{4\pi}\frac{Z}{\kappa(0)}\right]\left(1 + \frac{\omega Z}{4\pi\kappa_0}\right)^{-1}, \quad \kappa_0^2 = \frac{\omega^2}{c^2} - \frac{\mu^2}{R^2}. \qquad (12)$$

The parameter $|\mathscr{R}|^2$ characterises the reflectivity in power and the quantity $A = 1 - |\mathscr{R}|^2$ characterises the power absorbed in the plasma.

From expressions (11) and (12) we finally obtain

$$|\mathscr{R}|^2 = \left[\left(1 - \frac{\pi\eta\mu^2}{R^2\kappa_0}\right)^2 + \frac{\kappa_L^2}{\kappa_0^2}\frac{1}{\varepsilon}\right]\left[\left(1 + \frac{\pi\eta\mu^2}{R^2\kappa_0}\right)^2 + \frac{\kappa_L^2}{\kappa_0^2}\frac{1}{\varepsilon}\right]^{-1}. \qquad (13)$$

For invariable parameters of the problem employed in the numerical simulations, expression (13) can be rewritten in the form

$$|\mathscr{R}|^2 = \qquad (13a)$$

$$\frac{(1 - 2.61 L N_{\rm cr}/N)^2 (N/N_{\rm cr} - 1)^2 + 0.48 + 1.48(N/N_{\rm cr} - 1)}{(1 + 2.61 L N_{\rm cr}/N)^2 (N/N_{\rm cr} - 1)^2 + 0.48 + 1.48(N/N_{\rm cr} - 1)}.$$

Here, $N_{\rm cr} = 1.3 \times 10^{12}\ {\rm cm}^{-3}$ and L is measured in centimetres. Expressions (13) and (13a) are approximate: they are applicable only for $\lambda > L$, only for a monochromatic field (i.e. for an infinitely long pulse), and only in the linear approximation. Despite this fact, we shall use them when discussing the results of numerical simulations, which are free from the above restrictions.

3.2 Results of numerical simulations

As indicated above, the field was simulated by using the KARAT code [2], which was employed to solve the complete system of Maxwell equations, while the plasma was simulated by the PIC technique, which is a numerical realisation of the solution of the kinetic plasma model. That is why account is accurately taken of not only the geometry of the system, but also of the self-consistent nonlinear dynamics of electrons in the fields of the incident and reflected waves. The majority of calculations were carried out for numerical parameters when the Debye length was smaller than or of the order of the grid pitch; however, checking calculations showed that this fact had no effect on the results of simulations. All parameters of the system were analysed, but the pulse reflectivity was regarded as the main one. The reflection coefficients calculated for different parameter sets are collected in Table 1.

The data given in columns VII and VIII in Table 1 correspond to expressions (13). They should be compared in the first place with the data of numerical reflection simulations in the weak-field case (columns III and V) for a strong gradient corresponding to $L = 0 - 1.5$ cm. However,

Table 1. Reflection coefficients $\mathscr{R}$ for electromagnetic pulses for different parameter sets (columns I–VIII) of the system under study.

L/cm	Numerical simulation						Analytic calculation	
	I	II	III	IV	V	VI	VII	VIII
0	0.82	0.82	0.92	0.82	0.995	0.73	1.0	1.0
0.5	0.64	0.60	0.60	0.60	0.93	0.67	0.46	0.58
1.0	0.56	0.51	0.51	0.53	0.86	0.55	0.30	0.49
1.5	0.53	0.52	0.52	0.51	0.65	0.54	0.29	0.22
2.0	0.53	0.54	0.54	0.52	0.65	0.53	0.35	0.14
5.0	0.68	0.70	0.70	0.70	0.50	0.50	0.52	0.10
10.0	0.88	0.94	0.91	0.91	0.57	0.55	0.75	0.48
20.0	0.96	0.99	0.99	0.99	0.70	0.71	0.83	0.58

Note. For variants I and II, the field amplitude is $E = 5 \times 10^2$ V cm^{-1} for pulse durations $T = 0.2$ and 1 ns, respectively; for variants IV and V, 5×10^4 V cm^{-1} for $T = 1$ ns. The plasma density $n_e^{\max}$ is 2.5×10^{12} cm^{-3} (I–IV, VII) and 1×10^{13} cm^{-3} (V, VI, VIII).

even in this case a strong discrepancy is observed, which we attribute to the manifestation of plasma nonlinearity in the nonuniform field of the wave which experiences reflection. Electrons oscillate in the wave field of finite amplitude and, due to nonuniformity of the field, as if constitute a 'heated' plasma, in which there occur both the wave energy absorption and the production of the reflected wave.

Nonlinearity is somewhat different in character in the long-pulse case: due to the slowing down of the wave in the vicinity of the critical point, the field energy is accumulated and nonlinear oscillations appear once again, and therefore the energy is absorbed even for a low amplitude of the incident wave (see Table 1, columns III, V, and VI). In addition to the energy absorption of the reflected pulse at the critical point, this pulse is severely distorted. On the whole, the approximate theory is only qualitatively consistent with numerical simulations: the strongest absorption is observed for a wavelength comparable with the nonuniformity length L.

Consider the results of numerical simulations in greater detail.

Figure 3 shows three time dependences of the kinetic energy of plasma electrons for the maximum density equal to 2.5×10^{12} cm^{-3}. The dependence in Fig. 3a corresponds to the case when the nonuniformity length L exceeds the wavelength. In this case, the data for amplitudes of 5 and 5×10^4 V cm^{-1} are close and the electron energy vanishes upon reflection of the wave. For a strong gradient ($L =$ 5 cm) and a low field amplitude ($E = 5$ V cm^{-1}), the kinetic electron energy remains nonzero upon the reflection and oscillations are observed throughout the region occupied by the plasma. When the amplitude is increased to 5×10^4 V cm^{-1}, upon the reflection the kinetic energy of plasma electrons remains nonzero and is inherently thermal rather than oscillatory.

Figure 4 shows the time dependences of the magnetic and electric field energies for the maximum plasma density of 2.5×10^{12} cm^{-3}. One can see that for a strong gradient the oscillations of the electron plasma component are excited even in a low-amplitude field, which are not radiated and remain in the plasma.

Figures 5 and 6 show the phase portraits of the field at the instant of and after reflection of the wave. In the case of a small density gradient, the electrons experience an ordered, coherent motion in the wave field. This motion is observed both in front of the point of reflection (the critical point), where the incident field is weakly distorted, and behind the critical point, where the field decays exponentially. For a stronger gradient ($L = 5$ cm), the oscillation wavelength decreases as the plasma density increases.

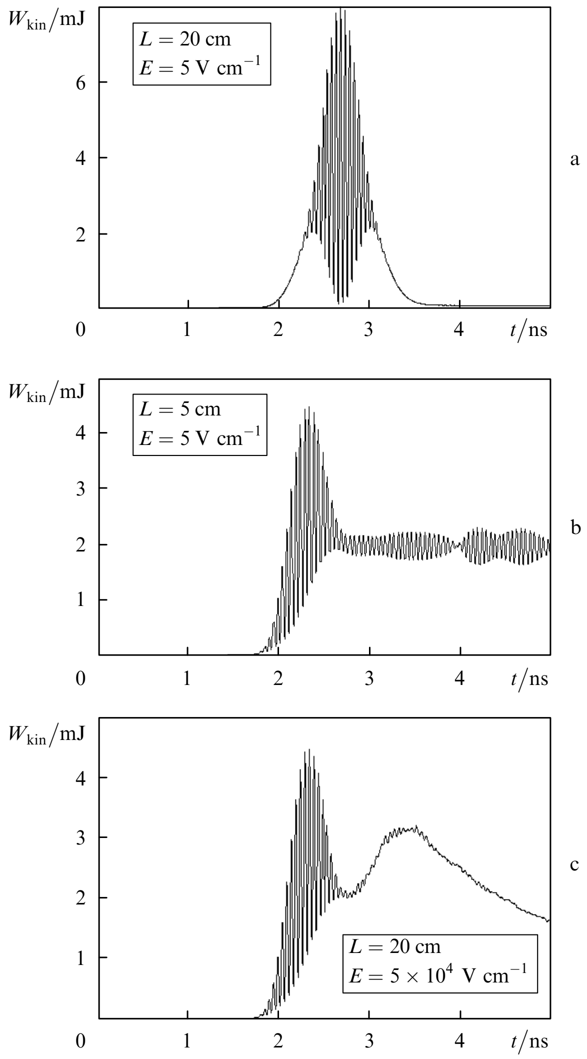

Figure 3. Time dependences of the electron kinetic energy W_{kin} for $N_{max} = 2.5 \times 10^{12}$ cm^{-3} and different values of L and E.

After the wave reflection (for $L = 20$ cm), the plasma remains cool, and therefore the phase plane is not depicted in this case. For a stronger gradient, the electrons gain energy, this energy being oscillatory in the low-field case, and these oscillations propagate into the plasma. In the case of higher-intensity field (5×10^4 V cm^{-1}), after the pulse reflection there are no oscillations and only the thermal electron motion is observed.

4. Discussion of results

We begin with the problem of pulse reflection from the supercritical waveguide taper, for which our numerical simulations yielded results coinciding with the results of the linear theory of reflection from a mirror. This comes as no surprise, because the taper length (40 cm) in this problem is much longer than the average wavelength of the incident radiation ($\lambda = 3$ cm) and its satellites (due to the finiteness of the pulse). As a consequence, the ray optics approx-

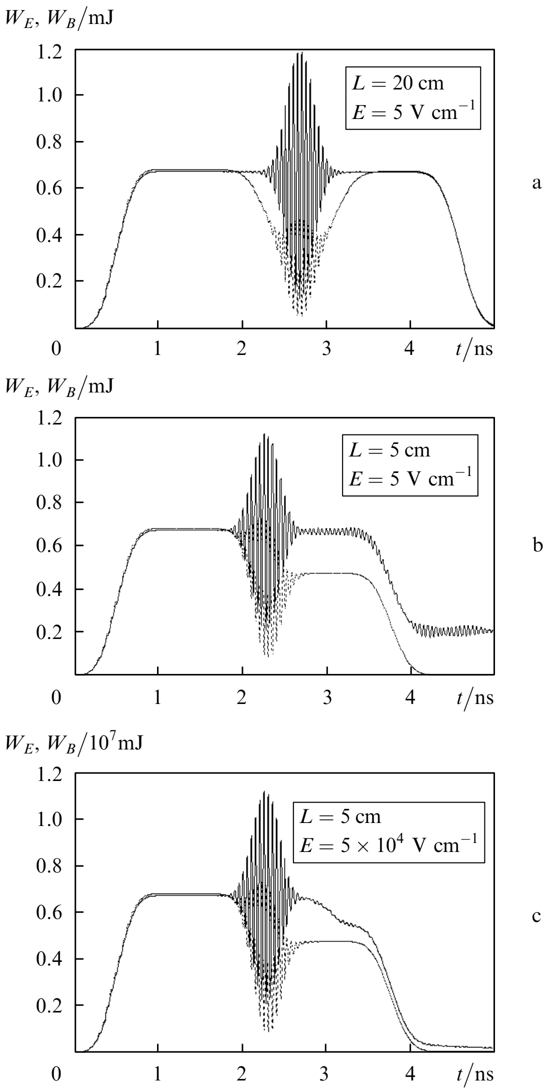

Figure 4. Time dependences of the total energies of magnetic (W_B) and electric (W_E) fields for $N_{\max} = 2.5 \times 10^{12}$ cm^{-3} and different values of L and E.

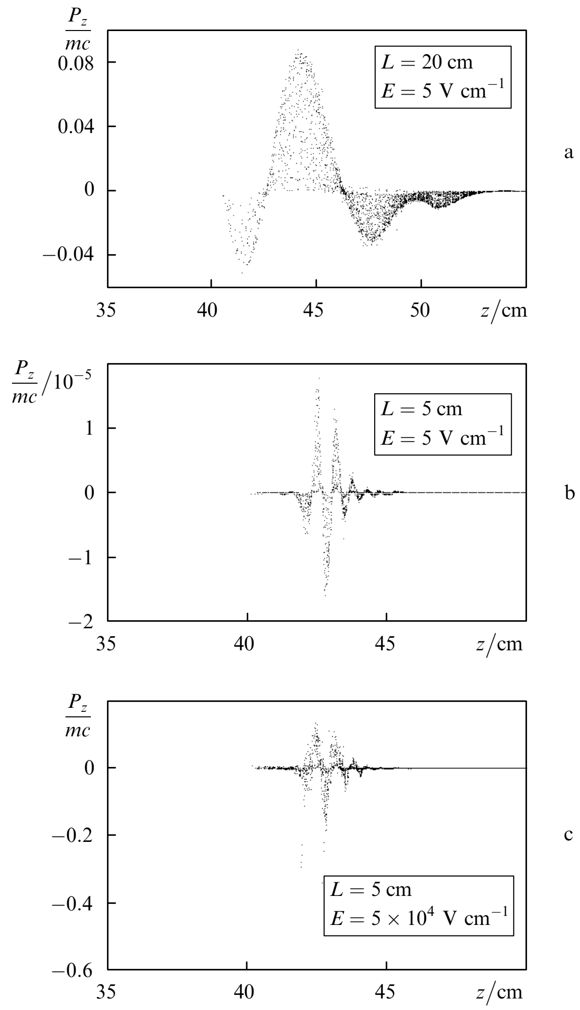

Figure 5. Phase plane of the plasma electrons at the instant of wave reflection for different values of L and E.

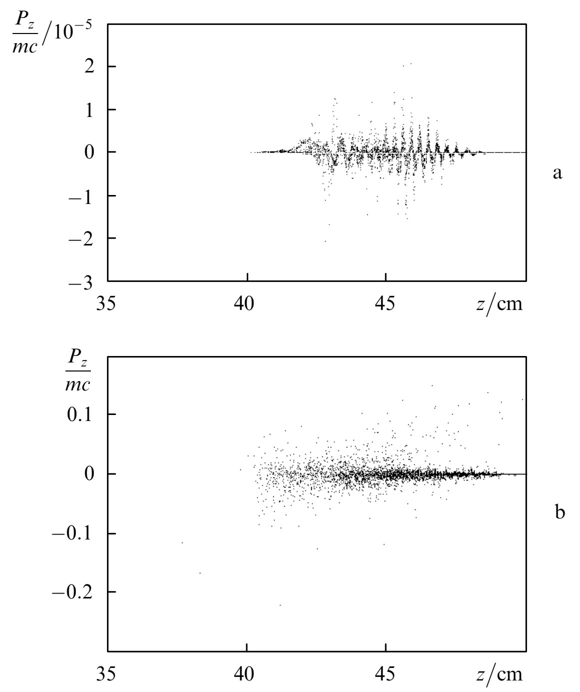

Figure 6. Phase plane of the plasma electrons upon wave reflection for different values of L and E.

imation can be used, which retains the shape of incident and reflected pulses to approximately within a factor $\lambda/L = 7\,\%$. Because the boundary conditions and the field equations themselves remained linear, there were no ground to expect the occurrence of nonlinear effects in the reflection problem.

The situation is different in the problem of pulse reflection from the plasma with a density increasing along the waveguide axis. In this case, there is only a qualitative agreement between the linear theory (columns VII and VIII in Table 1) and the numerical simulations: the highest-efficiency absorption of the incident radiation and a decrease of reflection are observed when $L \approx \lambda$, where λ is the in-plasma radiation wavelength, which strongly depends on the plasma density. The discrepancy between the approximate linear theory and the numerical simulations is, in our opinion, attributable to plasma nonlinearity. In particular, we attribute the discrepancy for $L = 0$ (reflection from the plasma with a sharp boundary) to the penetration of the incident wave field into the plasma. In the region located upstream of the critical point, this penetration takes place almost without distortions, behind this point it is attended with an exponential decay of the field intensity over a depth of c/ω_p, where ω_p is the Langmuir plasma frequency at the highest density. The nonuniform field with a finite amplitude results in nonuniform oscillations of the plasma electrons and the intersection of their trajectories, which shows up in the form of temperature changes and is responsible for the collisionless absorption of the wave field of the Landau damping type. This effect should become stronger with lowering n_{max} and increasing the amplitude of the incident wave, which follows from Table 1. Furthermore, this absorption should become stronger with increasing the pulse duration, because the effect of wave field accumulation at the critical point should manifest itself due to the lowering of group velocity. This effect is in turn equivalent to the increase of the wave amplitude and to the effect of 'thermal' absorption indicated above. Quite unexpected is the observation of strong absorption for a weak plasma density gradient ($L = 20$ cm), which contradicts both the above-outlined approximate theory and the ray optics. We believe that this is caused by the Landau damping over the long region of slowly varying field.

Finally, we draw attention to yet another quite serious discrepancy between the linear theory and the numerical simulations: in the theory, the absorption turns out to be stronger than in the simulations. This is due to the appearance of regular oscillations of plasma electrons in the incident wave field, which eventually come back in the form of radiation (backscattered incident radiation). This effect is not included in the theory, where any electron oscillations excited by the incident wave are associated with absorption. From the phase portraits of the fields and oscillations it is evident that regular electron oscillations do entail strong reflection. When the field and electron oscillations manage to become randomised, the absorption is strong and the reflection becomes low.

Therefore, the data obtained using numerical simulations and the linear theory differ primarily due to nonlinear effects. The latter should be significant when the electron oscillation velocity exceeds the thermal velocity, which we estimated on the basis of the intersection of electron velocities. For field amplitudes $E \sim 10^2 - 10^3$ V cm^{-1}, this estimate corresponds to a plasma temperature of $0.1 - 1$ eV. For $\upsilon_{T_e} \approx 3 \times 10^7$ cm s^{-1} (i.e. $T = 1$ eV), the condition

$$\frac{eE}{m\omega} \geqslant \upsilon_{T_e}$$

is fulfilled in the fields with intensities above 10^3 V cm^{-1}. Note that the above estimate of the nonlinearity threshold in the plasma is purely illustrative in character.

References

1. Rivlin L.A. *Kvantovaya Elektron.*, **36** (1), 90 (2006) [*Quantum Electron.*, **36** (1), 90 (2006)].
2. Tarakanov V. *User's Manual for Code KARAT* (Springfield, VA: Berkley Research Associates Inc., 1992).
3. Ginzburg V.L. *The Propagation of Electromagnetic Waves in Plasmas* (Oxford: Pergamon Press, 1970; Moscow: Nauka, 1967).
4. Al'pert Ya.L., Ginzburg V.L., Feinberg E.L. *Rasprostranenie radiovoln* (Propagation of Radiowaves) (Moscow: Fizmatgiz, 1967).
5. Gil'denburg V.B. *Zh. Eksp. Teor. Fiz.*, **41** (6), 1978 (1963).
6. Golant V.E., Piliya A.D. *Usp. Fiz. Nauk*, **104** (3), 413 (1971).
7. Erokhin N.I., Kuzelev M.V., Moiseev S.S., et al. *Neravnovesnye rezonansnye protsessy v plazmennoi radiofizike* (Nonequilibrium Resonance Processes in Plasma Radiophysics) (Moscow: Nauka, 1982).
8. Landau L.D., Lifshitz E.M. *Electrodynamics of Continuous Media* (Oxford: Pergamon Press, 1960, 1984; Moscow: Nauka, 1982).
9. Aleksandrov A.F., Rukhadze A.A. *Lektsii po elektrodinamike plazmopodobnykh sred* (Lectures on the Electrodynamics of Plasma-Like Media) (Moscow: Izd. MGU, 1999).